Experimental study of the effect of geodesic curvature on turbulent transport in magnetically confined plasma

PAPER • OPEN ACCESS

Experimental study of the effect of geodesic curvature on turbulent transport in magnetically confined plasma

View the article online for updates and enhancements.

Experimental study of the effect of geodesic curvature on turbulent transport in magnetically confined plasma

S Nishimoto[1,*] ⓘ, **K Nagaoka**[1,2] ⓘ, **M Nakata**[2,3] ⓘ, **S Yoshimura**[2] ⓘ, **K Tanaka**[2,4],
M Yokoyama[2,3], **M Nunami**[1,2], **T Tokuzawa**[2,3], **C Suzuki**[2,3] ⓘ, **R Seki**[2,3], **M Yoshinuma**[2,3],
G Motojima[2,3] ⓘ, **K Ida**[2,3] ⓘ and **Y Suzuki**[5] ⓘ

[1] Graduate School of Science, Nagoya University, Furo-cho, Nagoya, Aichi 464-8602, Japan
[2] National Institute for Fusion Science, Oroshi-cho, Toki, Gifu 509-5292, Japan
[3] The Graduate Institute for Advanced Studies, SOKENDAI, Oroshi-cho, Toki-shi, Gifu 509-5292, Japan
[4] Interdisciplinary Graduate School of Engineering Sciences, Kyushu University, Kasuga, Fukuoka 816-8580, Japan
[5] Graduate School of Advanced Science and Engineering, Hiroshima University, Higashi-Hiroshima 739-8527, Japan

E-mail: nishimoto.shu@nifs.ac.jp

CrossMark

Abstract

An experimental study has demonstrated the impact of the geodesic curvature of the magnetic field line on turbulent ion-heat transport in magnetically confined plasma using the large helical device. Statistical analyses with corrected Akaike Information Criterion and multiple regression have revealed that the geodesic curvature indicates a dominant contribution to the ion-heat transport. Geodesic curvature dependence of the zonal-flow effect is evaluated by using a gyrokinetic-simulation-based reduced model. Then, the analysis implies a significant enhancement of the zonal-flow effect with a small geodesic curvature. These two independent analyses indicated the possibility of external zonal-flow control with the geodesic curvature of the magnetic field.

Keywords: geodesic curvature, zonal flow, turbulent transport, fusion-burning plasma

1. Introduction

In magnetically confined plasmas, such as in tokamaks and helicals/stellarators, turbulent transport is one of the leading causes of plasma confinement degradation. The plasma pressure gradient excites drift-wave turbulence, for example,

the ion-temperature gradient (ITG) mode. Furthermore, turbulence drives particle and/or heat transport, mitigating the plasma-pressure gradient. Therefore, precise prediction of turbulent transport was required to study fusion-burning plasmas. Theoretical researches pointed out the improvement of the turbulence transport due to zonal flow, which is one of the mesoscopic coherent structures [1, 2]. The zonal flow has been experimentally identified in Compact Helical System with dual heavy ion beam probes, and the transport reduction due to zonal flow generation was confirmed experimentally [3, 4]. Then the zonal flow generation and the contribution to the reduction of turbulent transport have been intensively investigated in past decades. The nonlinear

gyrokinetic simulation showed reasonable agreement with the experimental observations [5], and it is widely recognized that the turbulent transport is dominated by co-existence of turbulence and zonal flow contributions. The prediction of turbulent transport in fusion burning plasma has been significantly progressed [6, 7]. The external control of turbulent transport is also important in addition to the control of magnetohydrodynamics (MHD) instabilities such as edge localized mode, resistive wall mode, and so on [8, 9].

On the other hand, turbulent transport modeling is a crucial issue in the optimization study of three-dimensional magnetic configuration for fusion-burning plasma confinement. There are no operational plasma devices that are optimized for turbulent transport. In a pioneering theoretical study, a proxy model was developed based on linear mixing diffusivity ($\chi_i \sim \gamma_k^{\mathrm{proxy}}/k_\perp^2$, where χ_i was ion heat transport coefficient, $\gamma_k^{\mathrm{proxy}}$ was a linear growth rate of the ITG mode or the trapped-electron mode, and $k_\perp$ was a wave number perpendicular to the magnetic field line) [10–12]. Using this linear proxy model, the turbulent transport level could be predicted by only linear calculation, which is suitable for the configuration optimization study. However, it is difficult to include the zonal-flow effect on the turbulent transport because nonlinear calculation is necessary to evaluate the zonal-flow level, which is unsuitable for the configuration optimization study due to too high calculation costs. Recently, a nonlinear proxy model, in which the zonal flow is taken into account was proposed [13]. The zonal flow was modeled as a function of geodesic curvature of the magnetic field line $\kappa_g = \boldsymbol{\kappa} \cdot (\nabla\psi/|\nabla\psi|) \times \boldsymbol{b}$, where $\boldsymbol{\kappa}$ was curvature of magnetic field defined as $\boldsymbol{\kappa} = \boldsymbol{b} \cdot \nabla\boldsymbol{b}$, $\boldsymbol{b}$ was a unit vector along the magnetic field, and ψ was poloidal flux. Therefore, turbulent transport level with the zonal flow can be calculated by only linear calculations. The zonal flow dependence on the geodesic curvature has been investigated with linear and nonlinear gyrokinetic simulations, in which the geodesic curvature was selectively modulated in the numerical simulations, and was verified for three different configurations such as the large helical device (LHD) NCSX-like, and axisymmetric configurations [13]. In tokamak geometry, the geodesic curvature tends to decrease with increasing elongation and increase with increasing triangularity [14]. To confirm the applicability of the nonlinear proxy model with zonal flow effect, experimental verification was required. In this study, the geodesic curvature dependence of ion heat transport on the LHD was investigated in two independent ways. One was a statistical analysis to clarify the ion heat transport dependence of the parameters. The second was the evaluation of zonal flow through the reduced ion-heat-transport model. Finally, the geodesic curvature dependence of zonal flow was discussed.

2. Plasma experiment

We experimented with the LHD, a heliotron-type superconducting plasma confinement device with a poloidal/toroidal mode number of $l = 2/m = 10$ [15]. The maximum magnetic field strength was 3 T. The major and minor radii were $3.5-4.0$ m and $0.6-0.65$ m, respectively. Three sets of poloidal
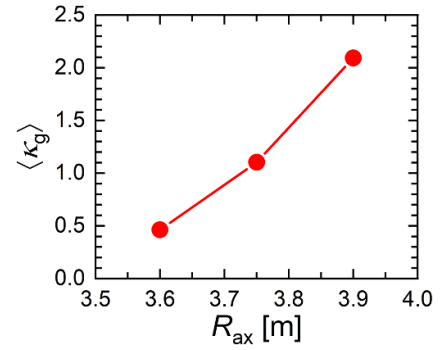

Figure 1. Flux-averaged normalized geodesic curvature weighted with Gaussian profile $\langle\kappa_g\rangle$ as a function of the radial position of magnetic axis R_{ax}.

coils can change the magnetic field configuration and the plasma position and shape change. In this study, we consider flux-averaged normalized geodesic curvature weighted with a Gaussian profile with a ballooning structure $\langle\kappa_g\rangle$ (detailed equation is in [16, 17]), which could have been significantly altered, as R_{ax} changes, as shown in figure 1. Regarding the LHD configuration, neoclassical transport and MHD stability depended on R_{ax}. Neoclassical transport was better in the inwardly shifted-configuration (small R_{ax}), and MHD stability was better in the outward-shifted one (large R_{ax}). In the early phase of the LHD project, it was found that plasma confinement was better with the inward-shifted configuration. However, the transport characteristics could not be explained by the nature of neoclassical transport [18]. The transport was considered to be dominated by turbulence. A gyrokinetic simulation with gyrokinetic Vlaosv simulation code (GKV) [5] showed zonal-flow enhancement with the inward-shifted configuration in the LHD and the suppression of turbulent transport [4]. Although plasma transport depended on some indices of the magnetic configuration, such as magnetic shear and helical ripples, in this study, we analyzed the transport characteristics by focusing on the geodesic curvature. We evaluated the effect of zonal flow on transport based on changes in R_{ax}.

The plasma experiment was carried out with three magnetic configurations of $R_{\mathrm{ax}} = 3.60$ m, 3.75 m, and 3.90 m with a magnetic field strength of $B = 2.631$ T and quadrupole component $B_{\mathrm{q}} = 100\%$. The plasma was produced by electron cyclotron heating and heated by neutron beam injection (NBI) [19] as well. Perpendicular NBI (NBI$_4$ and NBI$_5$) were modulated to measure the ion temperature using charge-exchange spectroscopy, as shown in figure 2(a). Electron temperature and density profiles were measured using a Thomson scattering system [20]. The profiles of the electron and ion temperatures and electron density were automatically calculated using AutoAna modules [21, 22]. The line-averaged density $\bar{n}_e$, the central density n_{e0} and the volume-averaged diamagnetic beta $\langle\beta_{\mathrm{dia}}\rangle$ are shown in figure 2(b). The central electron and ion temperatures and the temperature gradients at $r_{\mathrm{eff}}/a_{99} = 0.7$ are shown in figures 2(c) and (d), respectively, where r_{eff} is the effective minor radius, and a_{99} is the effective minor radius which encloses 99% of the total electron
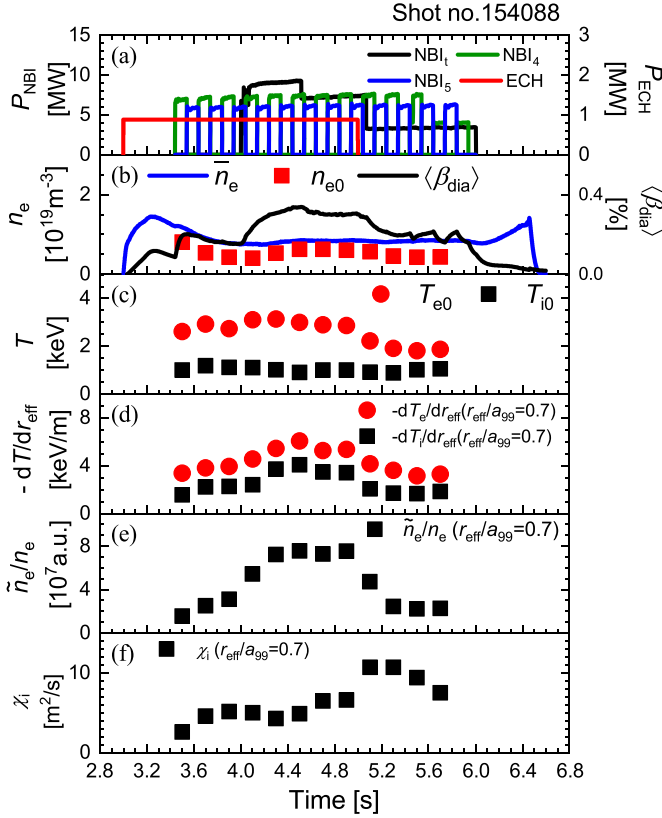
Figure 2. Typical discharge pattern of the LHD experiment. (a) Tangential NBI (NBI$_t$), perpendicular NBI (NBI$_4$ and NBI$_5$), and ECH port through power. (b) Line-averaged density $\bar{n}_e$, central density n_{e0} and volume-averaged diamagnetic beta $\langle \beta_{\mathrm{dia}} \rangle$. (c) Central-electron temperature T_{e0} and central-ion temperature T_{i0}. (d) Temperature gradient of electron $-dT_e/dr_{\mathrm{eff}}$ and ion $-dT_i/dr_{\mathrm{eff}}$ at $r_{\mathrm{eff}}/a_{99} = 0.7$. (e) Ion-scale density fluctuation normalized by electron density $\tilde{n}_e/n_e$ at $r_{\mathrm{eff}}/a_{99} = 0.7$. (f) Ion-heat transport coefficient χ_i at $r_{\mathrm{eff}}/a_{99} = 0.7$.

pressure. The ion-scale density fluctuation $\tilde{n}_e$ was measured using phase-contrast imaging [23], as shown in figure 2(e). The ion heat transport χ_i was evaluated by power balance analysis using TASK3D [24], which is also shown in figure 2(f).

3. Statistical analysis of ion heat transport

To investigate the parameter dependence of ion-heat transport, a database of heat transport was produced over the parameter regime as widely as possible, shown in figure 3. For simplicity, we discuss seven non-dimensional parameters at $r_{\mathrm{eff}}/a_{99} = 0.7$. The seven parameters, which are important for ion-turbulent transport were selected as ion-heat transport coefficient $\chi_i/\chi_i^{\mathrm{GB}} = \chi_i/(v_{T_i}\rho_i^2/R_{\mathrm{ax}})$ (where v_{T_i} and ρ_i are the ion-thermal velocity and ion-thermal gyroradius, respectively), normalized geodesic curvature $\langle \kappa_g \rangle / \langle \kappa_g \rangle^{\mathrm{ref}}$ ($\langle \kappa_g \rangle^{\mathrm{ref}} = 1.10$), temperature ratio T_e/T_i, normalized electron-temperature gradient $R/L_{T_e} (= -(R_{\mathrm{ax}}/T_e)\partial T_e/\partial r_{\mathrm{eff}})$, normalized ion-pressure gradient $R/L_n + R/L_{T_i} (= -(R_{\mathrm{ax}}/n_e)\partial n_e/\partial r_{\mathrm{eff}} - (R_{\mathrm{ax}}/T_i)\partial T_i/\partial r_{\mathrm{eff}})$, normalized density fluctuation $\tilde{n}_e/n_e$, normalized collisionality $\nu_{ii}^* = 4L\nu_{ii}/(3\sqrt{2\pi}v_{T_i})$
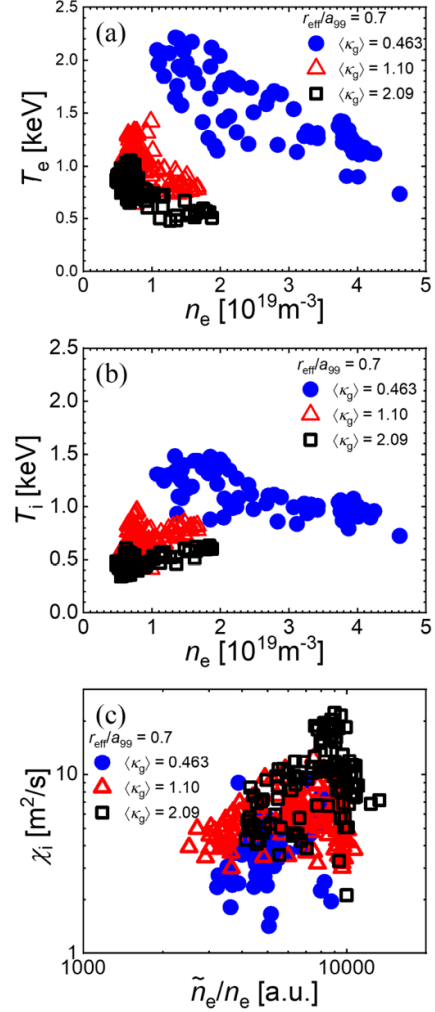

Figure 3. Plasma parameters at $r_{\mathrm{eff}}/a_{99} = 0.7$. (a) Electron density and electron-temperature space. (b) Electron density and ion-temperature space. (c) Ion-scale-density fluctuation normalized by electron density and ion heat-transport-coefficient space.

(where $L = qR_{\mathrm{ax}}/\epsilon^{3/2}$, with $q = 1.3$, $\epsilon = r_{\mathrm{eff}}/R_{\mathrm{ax}}$. $\nu_{ii} = n_e e_i^4 \ln\Lambda_{ii}/(8\sqrt{2}\pi \varepsilon_0^2 m_i^2 v_{T_i}^3)$, where $\ln\Lambda_{ii} = 17$). We applied the corrected Akaike Information Criterion (AICc) [25, 26] to $\chi_i/\chi_i^{\mathrm{GB}}(\langle \kappa_g \rangle/\langle \kappa_g \rangle^{\mathrm{ref}}, T_e/T_i, R/L_{T_e}, R/L_n + R/L_{T_i}, \tilde{n}_e/n_e, \nu_{ii}^*)$ for determination of the best parameter combination to characterize turbulent ion heat transport. The lowest AICc, which implies the best parameter combination, for each number of parameters (1, 2, ..., 6) is listed in table 1(a). Multi-regression analysis was applied to selected parameters power indices ($a_0, a_1, a_2, \ldots, a_6$) as $\chi_i/\chi_i^{\mathrm{GB}} = e^{a_0} x_1^{a_1} x_2^{a_2} \cdots$ are also listed in table 1(a). The $\langle \kappa_g \rangle/\langle \kappa_g \rangle^{\mathrm{ref}}$ was selected for all the parameters, and a positive correlation with the ion-heat transport was consistent with the theoretical prediction (at smaller geodesic curvature, the confinement is better). The best parameter combination was obtained with the lowest AICc value of 196.0 and was $\langle \kappa_g \rangle/\langle \kappa_g \rangle^{\mathrm{ref}}$, T_e/T_i, and $R/L_n + R/L_{T_i}$, and R/L_{T_e}. The T_e/T_i dependence indicated that the transport was apparently ITG driven. Surprisingly, $\tilde{n}_e/n_e$ was omitted. We discuss the reason for this later in the paper.

Table 1. Minimum AICc for each parameter number for (a) ion heat transport (χ_i/χ_i^{GB}) and (b) turbulent transport ($\chi_i^{turb}/\chi_i^{GB}$). The values in the parameter columns represent the exponents evaluated by multi-regression analysis for the selected parameter based on AICc.

(a) χ_i/χ_i^{GB}

Number of parameters	minimum AICc	a^0	$\langle \kappa_g \rangle / \langle \kappa_g \rangle^{ref}$	T_e/T_i	$R/L_n + R/L_{T_i}$	R/L_{T_e}	ν_{ii}^*	$\tilde{n}_e/n_e$
1	485.1	4.12	1.46					
2	338.5	3.52	1.25	1.43				
3	246.1	4.59	1.52	1.16	−0.439			
4	196.0	7.12	1.86	1.72	−0.484	−1.01		
5	197.1	7.05	1.79	1.76	−0.441	−0.995	0.0533	
6	199.2	6.96	1.79	1.75	−0.442	−1.00	0.0553	0.0128

(b) $\chi_i^{turb}/\chi_i^{GB}$

Number of parameters	minimum AICc	a^0	$\langle \kappa_g \rangle / \langle \kappa_g \rangle^{ref}$	T_e/T_i	R/L_{T_e}	$R/L_n + R/L_{T_i}$	$\tilde{n}_e/n_e$	ν_{ii}^*
1	624.6	3.79	1.85					
2	475.4	3.05	1.59	1.78				
3	459.8	5.07	1.84	2.27	−0.846			
4	453.7	5.69	1.97	2.21	−0.932	−0.168		
5	445.2	3.08	2.07	1.85	−1.17	−0.247	0.408	
6	446.2	3.40	2.16	1.82	−1.18	−0.308	0.376	−0.0843
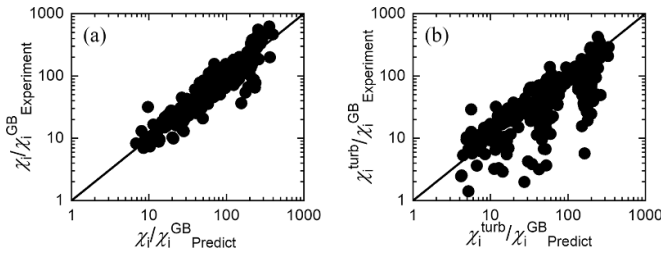
Figure 4. Comparison of experimental data and predicted data from multi-regression analysis in the case of (a) normalized ion-heat-transport coefficient, and (b) normalized-turbulent-transport coefficient.

We should consider the neoclassical transport contribution because the ε_{eff} also changed with the R_{ax} scan. Neoclassical transport χ_i^{NC} was evaluated using the local neoclassical transport code (GSRAKE) [27, 28], and the turbulent transport was evaluated by $\chi_i^{turb} = \chi_i - \chi_i^{NC}$. The same analysis was applied to the $\chi_i^{turb}/\chi_i^{GB}$ and the results are presented in table 1(b). Selected parameters for number 1 and number 2 were identical to those in table 1(a). The best parameter dependence obtained by the multi-regression analysis, when AICc is 445.2, was very similar to that for the χ_i/χ_i^{GB} although some minor differences were observed such as $\tilde{n}_e/n_e$.

On the other hand, the agreement of the multi-regression prediction was much better in the case of χ_i/χ_i^{GB} than in that of $\chi_i^{turb}/\chi_i^{GB}$, as shown in figure 4. The large deviation in $\chi_i^{turb}/\chi_i^{GB}$ was caused by an over-estimation of neoclassical transport with GSRAKE around the $E_r = 0$ region, which was pointed out in the comparison with a global neoclassical code (FORTEC-3D) [29]. To avoid this problem, further analysis was performed using χ_i/χ_i^{GB}, which was reasonable because the neoclassical contribution is generally small for the ion heat transport of the LHD plasma, typically less than 30% of the total ion heat transport.

4. Evaluation of zonal flow effect

Statistical analysis indicates the importance of the geodesic curvature for ion-heat transport, but does not explain the physical mechanism between them. Here, we discuss how the geodesic curvature affects the zonal flow. While direct measurement of zonal flow is difficult in LHD plasmas, the zonal-flow effect was evaluated with the reduced transport model, which was developed based on nonlinear gyrokinetic simulations with GKV and qualitatively verified by the LHD experiment [6]. The ion-heat transport in the reduced model was given by

$$\frac{\chi_i}{\chi_i^{GB}} = \frac{C_1 \mathcal{T}^\alpha}{C_2 + \mathcal{Z}^{1/2}/\mathcal{T}} \tag{1}$$

where $\mathcal{T}$ was the turbulence intensity, and $\mathcal{Z}$ was the zonal-flow intensity. For the LHD configurations, the coefficients were obtained as $C_1 = 6.3 \times 10^{-2}$, $C_2 = 1.1 \times 10^{-2}$, $\alpha = 0.38$ [6]. It should be noted that the zonal-flow-effect term $\mathcal{Z}^{1/2}/\mathcal{T}$, which suppressed ion-heat transport, could be evaluated by the ion heat transport χ_i and turbulence intensity. Both were obtained from LHD experiments.

To precisely evaluate the zonal-flow effect, the dependence of other parameters should be minimized. Therefore, we restricted the parameter regions as $0.9 \leqslant T_e/T_i \leqslant 1.3$, $8 \leqslant R/L_{T_e} \leqslant 14$, $-3 \leqslant R/L_n \leqslant 3.5$, $8 \leqslant R/L_{T_i} \leqslant 13$, and $9 \leqslant R/L_n + R/L_{T_i} \leqslant 14$, as shown in figure 5. The turbulence intensity $\mathcal{T}$ in equation (1) was normalized in the non-dimensional form as $\mathcal{T} = \frac{1}{2} \sum_{k_x,k_y \neq 0} \langle |\tilde{\phi}_{k_x,k_y}|^2 \rangle$, where $\tilde{\phi}$ was the normalized electrostatic potential fluctuation, and was
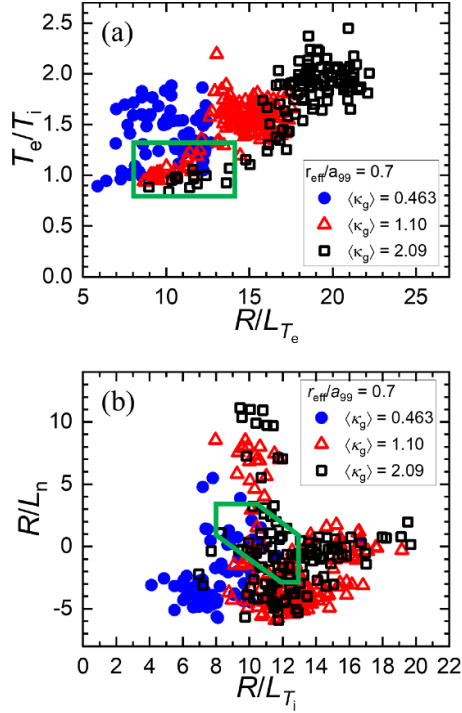
Figure 5. Distribution of the non-dimensional parameters in (a) T_e/T_i-R/L_{T_e} space and (b) R/L_n-R/L_{T_i} space. The green rectangle shows the selected parameter regimes as $0.9 \leqslant T_e/T_i \leqslant 1.3$, $8 \leqslant R/L_{T_e} \leqslant 14$, $-3 \leqslant R/L_n \leqslant 3.5$, $8 \leqslant R/L_{T_i} \leqslant 13$, and $9 \leqslant R/L_n + R/L_{T_i} \leqslant 14$.

Figure 6. Normalized ion-heat transport coefficient χ_i/χ_i^{GB}, and turbulence intensity $\mathcal{T}$ as a function of normalized-geodesic curvature ($\langle \kappa_g \rangle / \langle \kappa_g \rangle^{ref}$).

Figure 7. Zonal-flow effect $\mathcal{Z}^{1/2}/\mathcal{T}$ as a function of normalized-geodesic curvature ($\langle \kappa_g \rangle / \langle \kappa_g \rangle^{ref}$).

evaluated by the experimentally observed density fluctuation as $\mathcal{T} = \frac{1}{2}(\frac{R_{ax}}{\rho_i}\frac{\tilde{n}_e}{n_e})^2 \zeta$, where ζ was a calibration factor, and $\zeta = 4.5 \times 10^{-11}$ was obtained by a comparison between the experimental data and the nonlinear simulation results with GKV. The experimentally obtained data set of the ion-heat transport and turbulence intensity with almost the same non-dimensional parameters are summarized in figure 6. The ion heat transport tended to increase with the geodesic curvature and agreed well with the results of the statistical analysis (table 1(a)). However, the turbulence intensity does not show a clear power-law dependence. This is evidence of the small contribution of turbulence intensity to turbulent transport in the AICc analysis. Figure 7 shows the zonal-flow effect evaluated using equation (1) as a function of the geodesic curvature. The zonal-flow effect significantly decreases with the geodesic curvature, whereas the scatter is large in the region of $\mathcal{Z}^{1/2}/\mathcal{T} < C_2 = 1.1 \times 10^{-2}$. The dependence of the zonal-flow effect on the geodesic curvature is qualitatively consistent with the prediction of a numerical study, which investigated the geodesic curvature impact on the turbulent transport in the LHD configuration as well [13]. The zonal flow contribution with inwardly shifted configuration ($R_{ax} = 3.60$ m) was also pointed out by a nonlinear gyrokinetic simulation [4]. The consistency with simulation results
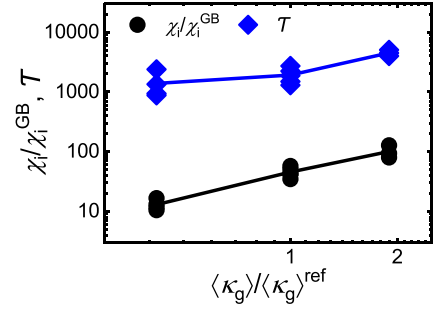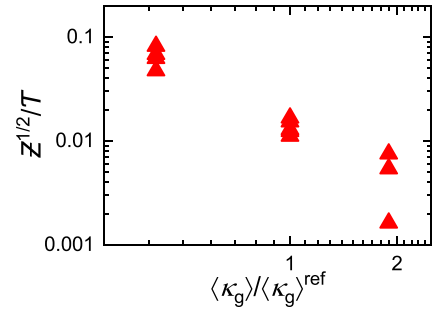
indicates that ion-heat transport suppression with the small geodesic curvature configuration is attributable to zonal-flow enhancement. It should be noted that when the zonal flow is enhanced, the transport decreased even when the turbulence was large, indicating a direct effect of the zonal flow to transport.

5. Conclusion

In this study, we experimentally investigated the geodesic curvature dependence of the zonal-flow effect in the LHD using two independent analyses. These analyses consistently indicate that the geodesic curvature significantly affects ion-heat transport through zonal-flow intensity. In general, the smaller geodesic curvature can reduce the radial excursion of trapped particles, and consequently the neoclassical transport. Nevertheless, it should be emphasized that the impacts of geodesic curvature on turbulent transport and zonal flows, which are evaluated by experiment data and theoretical model in this study, suggest many possibilities of a novel configuration optimization with activating zonal flows, regardless of detailed mechanisms in linear microinstabilites. This difference is very important from the turbulent transport optimization studies with linear growth rate calculation.

Data availability statement

Acknowledgment

ORCID iDs

S Nishimoto https://orcid.org/0009-0009-5097-6566
K Nagaoka https://orcid.org/0000-0002-5892-6047
M Nakata https://orcid.org/0000-0003-2693-4859
S Yoshimura https://orcid.org/0000-0002-0602-0665
C Suzuki https://orcid.org/0000-0001-6536-9034
G Motojima https://orcid.org/0000-0001-5522-3082
K Ida https://orcid.org/0000-0002-0585-4561
Y Suzuki https://orcid.org/0000-0001-7618-6305

References

[1] Rosenbluth M N and Hinton F L 1998 *Phys. Rev. Lett.* **80** 724–7
[2] Diamond P H, Itoh S-I, Itoh K and Hahm T S 2005 *Plasma Phys. Control. Fusion* **47** R35–R161
[3] Fujisawa A 2008 *Nucl. Fusion* **49** 013001
[4] Watanabe T-H, Sugama H and Ferrando-Margalet S 2008 *Phys. Rev. Lett.* **100** 195002
[5] Watanabe T-H and Sugama H 2005 *Nucl. Fusion* **46** 24
[6] Nunami M, Watanabe T-H and Sugama H 2013 *Phys. Plasmas* **20** 092307
[7] Nakayama T, Nakata M, Honda M, Narita E, Nunami M and Matsuoka S 2023 *Sci. Rep.* **13** 2319
[8] Hender T *et al* 2007 *Nucl. Fusion* **47** S128
[9] Leonard A W 2014 *Phys. Plasmas* **21** 090501
[10] Mynick H E, Pomphrey N and Xanthopoulos P 2010 *Phys. Rev. Lett.* **105** 095004
[11] Xanthopoulos P, Mynick H E, Helander P, Turkin Y, Plunk G G, Jenko F, Görler T, Told D, Bird T and Proll J H E 2014 *Phys. Rev. Lett.* **113** 155001
[12] Proll J H E, Mynick H E, Xanthopoulos P, Lazerson S A and Faber B J 2015 *Plasma Phys. Control. Fusion* **58** 014006
[13] Nakata M and Matsuoka S 2022 *Plasma Fusion Res.* **17** 1203077
[14] Beeke O, Barnes M, Romanelli M, Nakata M and Yoshida M 2021 *Nucl. Fusion* **61** 066020
[15] Iiyoshi A *et al* 1999 *Nucl. Fusion* **39** 1245–56
[16] Nakata M, Matsuyama A, Aiba N, Maeyama S, Nunami M and Watanabe T-H 2014 *Plasma Fusion Res.* **9** 1403029–1403029
[17] Nakata M, Honda M, Yoshida M, Urano H, Nunami M, Maeyama S, Watanabe T-H and Sugama H 2016 *Nucl. Fusion* **56** 086010
[18] Yamada H *et al* 2001 *Plasma Phys. Control. Fusion* **43** A55
[19] Iiyoshi A, Fujiwara M, Motojima O, Ohyabu N and Yamazaki K 1990 *Fusion Technol.* **17** 169–87
[20] Yamada I, Narihara K, Funaba H, Minami T, Hayashi H and Kohmoto T (LHD Experiment Group) 2010 *Fusion Sci. Technol.* **58** 345–51
[21] Emoto M, Ida K, Suzuki C, Yoshida M, Akiyama T, Nakamura Y, Sakamoto R, Yokoyama M and Yoshinuma M 2014 *Fusion Eng. Des.* **89** 758–60
[22] Emoto M, Suzuki C, Yokoyama M, Yoshinuma M, Seki R and Ida K 2018 *Fusion Sci. Technol.* **74** 161–6
[23] Tanaka K, Michael C A, Vyacheslavov L N, Sanin A L, Kawahata K, Akiyama T, Tokuzawa T and Okajima S 2008 *Rev. Sci. Instrum.* **79** 10E702
[24] Yokoyama M, Wakasa A, Seki R, Sato M, Murakami S, Suzuki C, Nakamura Y, Fukuyama A and Group L E 2012 *Plasma Fusion Res.* **7** 2403011
[25] Akaike H 1974 *IEEE Trans. Autom. Control* **19** 716–23
[26] Sugiura N 1978 *Commun. Stat. - Theory Methods* **7** 13–26
[27] Beidler C D and D'haeseleer W D 1995 *Plasma Phys. Control. Fusion* **37** 463
[28] Beidler C D and Maaßberg H 2001 *Plasma Phys. Control. Fusion* **43** 1131–48
[29] Matsuoka S, Satake S, Kanno R and Sugama H 2015 *Phys. Plasmas* **22** 072511